

PHYSICAL REVIEW B

CONDENSED MATTER

THIRD SERIES, VOLUME 49, NUMBER 9

1 MARCH 1994-I

X-ray absorption, emission, and resonant inelastic scattering in solids

Yanjun Ma*

*Physics Department, University of Washington, Seattle, Washington 98195
and Molecular Science Research Center, Pacific Northwest Laboratories, Richland, Washington 99352*

(Received 3 August 1993)

The process of x-ray absorption and emission in solids is considered as an x-ray resonant inelastic scattering process. This coherent inelastic scattering picture has recently been used to interpret the excitation energy dependence in the x-ray emission spectra excited with synchrotron radiation. It also suggests that with near threshold excitation, the x-ray emission spectra should be spatially anisotropic. We consider the validity and implication of this approach and factors affecting the spatial and temporal coherence in the scattering process. Taking into account the relaxation effects such as the electron-electron and the electron-phonon interactions, a significant fraction of the total emission intensity may be attributed to the coherent scattering. This picture of the x-ray absorption and emission process opens up the possibility for *momentum-resolved* x-ray absorption and emission measurements that can be used for band-structure determination. In addition, it has important implications on the fluorescence yield method of obtaining the absorption spectra.

I. INTRODUCTION

X-ray absorption and emission in solids have been traditionally treated as two related yet independent processes, with the absorption and emission spectra providing information on the unoccupied and occupied electronic states, respectively.¹ The origin for this traditional view is mostly historical: due to the experimental limitations the absorption and emission spectra are usually obtained independent of each other. Recent experimental advances, especially the availability of intense x-ray beams from synchrotron radiation, made it possible to perform the absorption and emission spectra measurements in the same experiments.^{2,3} Consequently, it is worthwhile to review our understanding of the absorption and emission processes, especially their interrelationship, which might have significant consequences on their use as probes of electronic structure of matter. Recently, C K-emission spectra of diamond were shown to be strongly dependent on the energy of the excitation photons.⁴ It was proposed that this excitation energy dependence is evidence for coherent inelastic scattering of x rays in crystalline solids, i.e., the absorption-emission process should be treated as a single inelastic scattering process with well-defined crystal momentum conservation. As a consequence, the emission spectrum reflects the valence-band density of states (DOS) sampled in a restricted region of the Brillouin zone (BZ) that is determined by the absorption process. Band-structure calcula-

tions based on the scattering picture produced results that closely resemble those obtained in the experiment.⁵ Si L-emission measurements also provided evidence supporting this inelastic scattering interpretation. While the emission spectra of crystalline Si show dramatic excitation energy dependence,⁶ no excitation energy dependence has been observed for amorphous Si,⁷ suggesting that the long-range crystalline order is the cause for the excitation energy dependence. The discovery that x-ray absorption (XAS) and emission (XES) spectroscopies can provide momentum-resolved electronic density-of-states information is very surprising. Since localized core electrons are involved in these processes, it was traditionally believed that only the DOS integrated over all the BZ can be obtained.¹ Equally surprising is the coherence between the absorption and the emission processes.

In this paper we will discuss in detail the absorption-emission process in condensed systems: the resonant inelastic scattering description, its validity, and implications. It will be clear from the discussion that the coherence between the emission and absorption is a consequence of the fast decay process, while the momentum conservation is due to the delocalization of the electron-hole pair of the final state. The localized core hole potential will affect the momentum resolution of the scattering process to a limited extent. The relaxation processes, such as those due to the electron-phonon and electron-electron interactions, will affect the coherence between the absorption and emission and make incoherent contri-

butions to the scattering cross section. However, the coherent scattering is generally a significant contribution and its use as a new band determination technique should be explored.

In the following section, we will first discuss the scattering process in the independent particle picture. The implications and complications due to many particle interactions will be discussed in Sec. III. We will conclude in Sec. IV.

II. SINGLE-PARTICLE THEORY

The interaction of photon with matter is determined by the following interaction Hamiltonian:

$$H_1 = \frac{e}{mc} \mathbf{p} \cdot \mathbf{A} + \frac{e^2}{2mc^2} \mathbf{A} \cdot \mathbf{A}. \quad (1)$$

As is well known, the $\mathbf{p} \cdot \mathbf{A}$ term describes one-photon processes, i.e., the absorption or the emission of a single photon. The $\mathbf{A} \cdot \mathbf{A}$ term describes two-photon processes such as diffraction and inelastic scattering. In this paper, we will concentrate on the process generated by the $\mathbf{p} \cdot \mathbf{A}$ term in the *second order*, i.e., a process involving multiple absorption and emission processes.

In a typical x-ray inelastic scattering experiment the incident photons with energy $\hbar\omega_1$ impact on a sample and the scattered photons with energy $\hbar\omega_2$ are monitored with energy analyzer-spectrometer. The scattering cross section can be derived from the Born approximation as⁸

$$\frac{d\sigma}{d\Omega} \propto \sum_f \left| \left\langle f \left| \frac{e^2}{2mc^2} \mathbf{A}_2 \cdot \mathbf{A}_1 \right| i \right\rangle + \frac{e}{mc} \sum_m \left[\frac{\langle f | \mathbf{p} \cdot \mathbf{A}_2 | m \rangle \langle m | \mathbf{p} \cdot \mathbf{A}_1 | i \rangle}{E_m - E_i - \hbar\omega_1 - i\Gamma_m/2} + \frac{\langle f | \mathbf{p} \cdot \mathbf{A}_1 | m \rangle \langle m | \mathbf{p} \cdot \mathbf{A}_2 | i \rangle}{E_i - E_m + \hbar\omega_2} \right] \right|^2 \delta(\omega_1 - \omega_2 - \omega_{fi}), \quad (2)$$

where the first term gives rise to the normal inelastic scattering,⁹ and the other two terms describe the anomalous inelastic scattering of the x-ray photon, and $\hbar\omega_{fi} = E_f - E_i$. These scattering processes are illustrated graphically in Fig. 1. The sum over m is for all the possible intermediate states (with lifetime Γ_m). When $\hbar\omega_1$ is at or above an absorption threshold, the resonant term dominates by an order of $[\hbar(\omega_1 - \omega_2)/\Gamma_m]^2$. In this paper, we will discuss only the resonant process, where the electron from a core level, by the absorption of the incident photon, is excited to an unoccupied state, followed by the decay of a valence electron into the core hole, emitting a photon of $\hbar\omega_2$. This is the process measured in the photon excited x-ray emission experiments. It is essentially the resonant Raman scattering process (RRS).¹⁰ However, the x-ray RRS usually refers to excitations just below the absorption threshold and is usually associated with scattering from bound states. Above the absorption threshold, it was generally believed that the inelastic scattering process is divided into two independent, absorption followed by emission, processes where the transition rate is the product of the absorption and emission transition rates.¹¹ Recent experiments clearly

showed that this ‘‘absorption followed by emission’’ picture is inadequate, and that there is coherence between the absorption and emission processes.^{4,6,7} We therefore call this process, where the final-state electron-hole pair is delocalized, by a more general term: x-ray resonant inelastic scattering (XRIS).

We consider the XRIS from crystalline solids. In the single-particle picture, the ground-state wave function is a Slater determinant with the electrons filled to the valence-band maximum or the Fermi level. The final state has a conduction electron in the previously unoccupied state with crystal momentum \mathbf{k}_1 and an electron missing from the valence state at \mathbf{k}_2 . These variables are determined by the photon energy, momentum, and the band structure of the solid. The intermediate state of the resonance is characterized by a hole in the core state $|c\rangle$ with energy ε_c , a photoelectron in $|e^*\rangle$ and energy ε_e . The decay of the core state is by transition of a valence electron from $|h^*\rangle$ and energy ε_h , to the core hole, where $*$ denotes the excited states. Substituting these functions into Eq. (1), the resonant scattering term becomes

$$\frac{d\sigma}{d\Omega} \propto \sum_{\mathbf{k}_1, \mathbf{k}_2} \left| \sum_{c, e, h} \frac{\langle \mathbf{k}_1 | e^* \rangle \langle h^* | \mathbf{k}_2 \rangle \langle c | \mathbf{p} \cdot \mathbf{A}_2 | h^* \rangle \langle e^* | \mathbf{p} \cdot \mathbf{A}_1 | c \rangle}{\varepsilon_c - \varepsilon_e - \hbar\omega_1 - i\Gamma_c/2} S^2 \right|^2 \delta(\omega_1 - \omega_2 - \omega_{fi}). \quad (3)$$

S denotes the overlap integral for all the electrons that did not participate in the transitions. Normally near an absorption edge $S=1$ while at higher energies S could be less than one, with the multielectron processes taking away the spectral weight.¹² Neglecting the effect of the core hole on the wave functions for the moment, all the single-particle wave functions are then Bloch wave functions,¹³ characterized by their crystal momenta. From the orthogonality condition, we have, e.g., $\langle \mathbf{k}_1 | e^* \rangle = \delta_{\mathbf{k}_1, \mathbf{k}_e}$, where \mathbf{k}_e is the momentum of the photoelectron. Also, since the core wave function is localized, it can be written in the tight-binding form $|c\rangle = \sum_{\mathbf{R}} e^{i\mathbf{k}_c \cdot \mathbf{R}} \varphi_c(\mathbf{r} - \mathbf{R})$, where φ_c is the atomic core wave func-

tion located at \mathbf{R} , e.g., the Cl s for diamond. The energy of the core level ϵ_c is essentially a constant, independent of the position \mathbf{R} and the momentum \mathbf{k}_c , the sum over \mathbf{k}_c can then be replaced by the sum over the lattice site \mathbf{R} by using $\sum_{\mathbf{k}_c} e^{i\mathbf{k}_c(\mathbf{R}-\mathbf{R}')} = N\delta_{\mathbf{R}\mathbf{R}'}$. Substituting these results, the photon amplitudes, e.g., $\mathbf{A}_1 = A_0 \mathbf{e}_1 e^{i\mathbf{q}_1 \mathbf{r}}$ with \mathbf{e} the polarization vector, and the Bloch wave functions, $|e^*\rangle = e^{i\mathbf{k}_e \cdot \mathbf{r}} u_e(\mathbf{r})$ and $|h^*\rangle = e^{i\mathbf{k}_h \cdot \mathbf{r}} u_h(\mathbf{r})$, into Eq. (3), we obtain a cross section for the XRIS as

$$\frac{d\sigma}{d\Omega} \propto \sum_{\mathbf{k}_h} \left| \sum_{\mathbf{k}_e} M_{c,h} \frac{M_{e,c}}{\epsilon_e(\mathbf{k}_e) - \epsilon_c - \hbar\omega_1 - i\Gamma/2} \sum_{\mathbf{R}} e^{i\mathbf{R} \cdot (\mathbf{q}_1 - \mathbf{q}_2 + \mathbf{k}_h - \mathbf{k}_e)} \right|^2 \delta(\omega_1 - \omega_2 - \omega_{fi}) . \quad (4)$$

In the dipole approximation, the matrix elements are, e.g., $M_{e,c} = \int u_e \mathbf{p} \cdot \mathbf{e}_1 \varphi_c d^3r$. As expected, in Eq. (4) the first two terms describe the resonant absorption process followed by emission on the *same* atom, as required by the localized core hole. The energy and momentum of the electron \mathbf{k}_e in the final state is that determined by the resonance condition in the absorption process,

$$\epsilon_e(\mathbf{k}_e) - \epsilon_c = \hbar\omega_1 . \quad (5)$$

The energy ϵ_h is determined by the overall energy conservation, $\epsilon_e - \epsilon_h = \hbar\omega_1 - \hbar\omega_2$, or

$$\begin{aligned} \hbar\omega_2 &= \epsilon_e(\mathbf{k}_e) - \epsilon_c - \epsilon_e(\mathbf{k}_e) + \epsilon_h(\mathbf{k}_h) \\ &= \epsilon_h(\mathbf{k}_h) - \epsilon_c , \end{aligned} \quad (6)$$

which is just the result for the normal x-ray emission process.

What is unusual in Eq. (4) is the sum over the atomic positions, \mathbf{R} . This sum gives rise to a crystal momentum conservation, $\mathbf{q}_1 - \mathbf{q}_2 = \mathbf{k}_e - \mathbf{k}_h + \mathbf{G}$, which relates momentum of the electron-hole pair to the momentum transfer from the photons, obtained from

$$\sum_{\mathbf{R}} e^{i\mathbf{R}(\mathbf{q}_1 - \mathbf{q}_2 + \mathbf{k}_h - \mathbf{k}_e)} = N\delta_{\mathbf{q}_1 - \mathbf{q}_2 + \mathbf{k}_h - \mathbf{k}_e, \mathbf{G}} , \quad (7)$$

where \mathbf{G} is a reciprocal lattice vector. Note that the sum is over the coherent region of the photon field, and it resembles the structure factor in the x-ray diffraction process. In fact, if we let $\mathbf{k}_h = \mathbf{k}_e$ and $u_e(\mathbf{r}) = u_h(\mathbf{r})$, Eq. (4) simply describes the anomalous *elastic* scattering of x rays. In this case the momentum conservation is $\mathbf{q}_1 - \mathbf{q}_2 = \mathbf{G}$, i.e., the Bragg condition. Therefore, we may interpret the resonant inelastic scattering as a generalization of the anomalous scattering: instead of the ground state, the final state of the solid is an excited, charge-

density-wave-like state composed of the electron-hole pair. Thus, XRIS is a part of the anomalous *inelastic* scattering of x rays.

The comparison with the elastic anomalous scattering, where a core electron is momentarily excited to the continuum and the same electron recombines with the core hole, also suggests the following interpretation for the resonant inelastic scattering in solids. The core electron is well known to be localized. Therefore, the absorption and emission process should occur on individual atoms. Equation (4) and the momentum conservation comes from the summation of the coherent absorption and emission events among all the equivalent atoms within the coherent x-ray fields. The absorption and emission processes are coherent, contributing factors of $e^{i\mathbf{R}(\mathbf{q}_1 - \mathbf{k}_e)}$ and $e^{-i\mathbf{R}(\mathbf{q}_2 - \mathbf{k}_h)}$ to the overall scattering process, respectively. Also, the transition processes occurred on different, but equivalent, atoms are coherent. In other words, there exists both temporal (between absorption and emission) as well as spatial (between equivalent atoms within the coherent photon fields) coherence.

The above picture can also be applied to groups of equivalent atoms such as molecules and clusters. Instead of Bloch wave functions, molecular wave functions such as linear combination of atomic orbitals (LCAO) are substituted in Eq. (3). Recent excitation energy dependence observed in the CK emission of C_{60} may indeed be due to such coherent scattering.¹⁴

The polarization dependence in the resonance scattering process and its use for studying the magnetic properties merit special mention. As can be derived from Eq. (3), the magnetic quantum number selection rule for the absorption and emission processes are $m_c - m_e = m_{q_1}$ and $m_h - m_c = -m_{q_2}$. Where m_{q_1} and m_{q_2} are the quantum number of the photons, e.g., $m_{q_1} = 1, 0, -1$ for left circularly, linear, and right circularly polarized light, respectively. For the overall scattering process, $m_h - m_e = m_{q_1} - m_{q_2}$. Therefore, by using differently polarized excitation and polarization analysis of emitted radiation, angular momentum information of either the conduction band or the valence band can be obtained. This relation will be useful to study the electronic structures of magnetic systems.

III. DISCUSSIONS

This new understanding of the x-ray absorption and emission process in solids has very profound and observable consequences. The first consequence of Eq. (4) is that x-ray emission of the valence band is excitation ener-

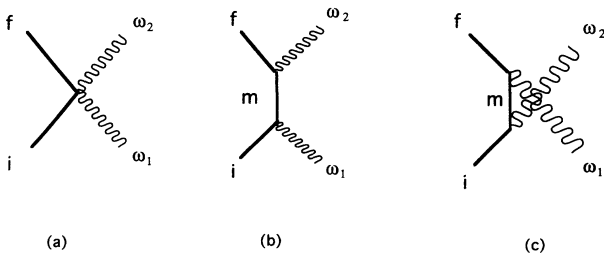


FIG. 1. Graphical illustration of the photon scattering processes described by Eq. (2): normal inelastic scattering (a), resonant (b), and nonresonant (c) anomalous scattering.

gy dependent. Depending on the band structure, the momentum of the electron in the final state is a function of the incident photon energy through the resonant condition, Eq. (5). Only emission from $\mathbf{k}_h = \mathbf{q}_2 - \mathbf{q}_1 + \mathbf{k}_e$ and $\epsilon_h(\mathbf{k}_h) = \epsilon_c + \hbar\omega_2$ of the valence band is allowed. Therefore, as $\hbar\omega_1$ is varied, the emission *spectral line shape* will vary, with enhanced emission from a region or regions of the BZ determined by the energy and momentum conservation. It should be emphasized that the prediction is for the variation of spectral shape, other than the total emission intensity which will also vary with the absorption cross section at different incident energies.

This prediction has been confirmed by recent experiments at the C *K* edge of diamond,⁴ and the Si *L* edge of crystalline Si.^{6,7} In these soft x-ray experiments, the wavelength of the photons are much longer than the lattice constants of the solids. The momentum transfer from the x ray to the sample is negligible. Consequently, the momentum conservation is reduced to $\mathbf{k}_h = \mathbf{k}_e$. Thus, the net effect of the two core transitions is a vertical transition with a conduction electron and a valence hole, much like an optical or UV transition. Simple tight-binding calculations based on this vertical transition rule yielded results in very good agreement with the experimental results.⁵ More recently, a similar excitation energy dependence was observed in the C *K*-emission spectra of graphite.¹⁵

At x-ray wavelength comparable to lattice spacings, Eq. (4) predicts that x-ray emission from the valence band is spatially anisotropic. When $\hbar\omega_1$ and $\hbar\omega_2$ are fixed, changing the direction of the detection will vary \mathbf{q}_2 , thus the momentum of the valence hole created in the emission process. Therefore, the emission spectra shape will vary as the detection angle. Indeed, recent measurements show that, under identical experimental conditions, the *K β* emission spectra of silicon obtained with near threshold excitations are very different for (100), (110), and (111) orientations.¹⁶

These properties of XRES provided the basic principle for performing *momentum-resolved* XAS and XES measurements. Since the momentum of both the incident and emitted photon can be obtained from their energy and direction, if one of the electronic momentum can be obtained, the other is known. For example, with the incident photon energy fixed at an absorption threshold, e.g., the *K* edge of Si, the photoelectron is excited to the bottom of the conduction band at \mathbf{k}_{\min} . It is then possible to map the valence band $\epsilon_h(\mathbf{k}_h)$ through angle-resolved XES, where the enhancement in the emission spectrum determines the energy and the crystal momentum is obtained from $\mathbf{k}_h = \mathbf{q}_2 - \mathbf{q}_1 + \mathbf{k}_{\min}$. On the other hand, one can perform partial fluorescence yield measurement of the absorption spectrum by monitoring the emission from a high density-of-states point \mathbf{k}_0 in the valence band. The absorption spectrum obtained this way contain only the information on the unoccupied states at momentum $\mathbf{k}_e = \mathbf{q}_1 - \mathbf{q}_2 + \mathbf{k}_0$ which can be varied by either changing the sample orientation or the direction of the photons.

It was estimated that the coherent scattering contributed to about 30–50 % of the total detected emission intensity in diamond.^{4,5} We now discuss the origin of the in-

coherent contribution as well as the validity of the coherent scattering approach. Clearly, the prerequisite for the momentum conservation relation is that the electron-hole pair in the final state have well-defined crystal momentum. This is reflected in the use of Bloch wave functions for the electron-hole pair in deriving Eq. (4). Thus, it is most important to identify the interactions which may cause the localization (delocalization in the reciprocal space) of the electron-hole pair. Since the core hole is localized, the effect of the core-hole potential is expected to be the most important. This was the main reason for the traditional belief that no electronic momentum information can be extracted from the core-level techniques.¹

The effect of the core-hole potential on the electronic wave functions of the conduction band has been well treated in the theory of excitons, especially that of core excitons.¹⁷ In the presence of the core hole, the photoelectron may be described by a wave packet around the core hole. Its wave function may be expanded from Bloch wave function: $|e^*\rangle = \sum_{\mathbf{k}} A(\mathbf{k} - \mathbf{k}_e)|\mathbf{k}\rangle$. Therefore, we need to replace $\langle \mathbf{k}_1 | e^* \rangle$ in Eq. (3) by the more general form: $A(\mathbf{k}_1 - \mathbf{k}_e)$. It can then be seen that instead of a single Bloch wave, the electron in the final state is now a superposition of many Bloch waves, determined from the envelope function $A(\mathbf{k})$. In most cases, for excitations above the band gap, the effect of the core-hole potential on the conduction- or valence-band wave functions is small, $A(\mathbf{k}) \approx \delta(\mathbf{k} - \mathbf{k}_e)$ and we recover the earlier results. In the other limits, when (1) the photon electron is excited into a localized orbital and (2) electron in the emission process is from a localized deep core level, $\langle \mathbf{k}_1 | e^* \rangle$ or $\langle \mathbf{k}_2 | h^* \rangle \approx 1$. The whole BZ has to be sampled in Eq. (4). No electronic momentum information can then be resolved from this type of scattering process. We will have the normal isotropic fluorescence.

In the intermediate case, for example, when the incident photon energy corresponds to the excitation of a shallow core exciton, the photoelectron wave function is composed of wave functions at around, e.g., the conduction-band minimum \mathbf{k}_{\min} . Assuming a Gaussian envelope function, the size of this region is then roughly $2\pi/D$, where D is the size of the exciton. The result will be to add this amount of uncertainty to the momentum-conservation relation, which ultimately contributes to the momentum resolution that can be achieved in the scattering experiment.

A special case is when the incident photon energy corresponds to the creation of a core exciton. In this case, the energy of the emitted photon will be different from that in the normal emission process. This is because during the emission transition which eliminated the core hole, the photoelectron changes from that of the core exciton state to a valence exciton state near the minimum of the conduction band. Using $\hbar\omega_2 = \epsilon_h - \epsilon_c^* + \epsilon_e^* - \epsilon_e$, the emission spectrum is shifted by approximately $\epsilon_{\min} - \epsilon_e^*$, to lower photon energy. This kind of shift has been observed in the B *K*-emission spectra of B_2O_3 and BN.¹⁸ From the above discussion we note that it may be possible to use the scattering technique to extract the exciton envelope function $|A(\mathbf{k})|^2$.

The above discussions are related to the spatial coherence of the absorption and emission processes where the coherence length of the photon and the size of the excitonic effect contribute to the momentum resolution of the scattering. We now discuss the temporal coherence, i.e., the coherence between the absorption and emission processes. In Eq. (3), the same intermediate wave function is used in the absorption and the emission matrix elements. This is true if the relaxation time of the system is much less than the lifetime of the intermediate state. If there is complete relaxation, the absorption and the emission should then be treated as two independent processes. There are several important time scales in the scattering process: lifetime of the intermediate state \hbar/Γ_c , the phonon relaxation time $1/\omega_D$ (where ω_D is the Debye frequency), and the lifetime of the photoelectron \hbar/Γ_e . Clearly, the coherence condition is $\Gamma_c \gg \Gamma_e, \hbar\omega_D$. The effect of the photoelectron scattering due to phonons and impurities can be controlled by measuring at low temperature and the use of high-quality samples, while for insulators the scattering by electrons are not very strong because the finite band gaps prevent the creation of electron-hole pairs. For example, for diamond the energy gap is 5.5 eV. Only when the photoelectron has energy of more than 5.5 eV can the e - e scattering be important. For insulators and semiconductors, the most important relaxation mechanism is clearly the phonon relaxation: because of the excitation involves the localized core state, electron-phonon coupling through the Franck-Condon process is always present.

The effect of the phonon relaxation in the x-ray absorption and emission process has been well studied.¹⁹ It was found that the phonon relaxation is not complete at least up to $\Gamma_c \sim \hbar\omega_D$. For diamond, $\Gamma_{1s} \approx \hbar\omega_D \approx 0.2$ eV. Thus, one may estimate that up to $e^{-\hbar\omega_D/\Gamma_{1s}} \approx 40\%$ of the emission intensity is due to the coherent scattering. This order of magnitude estimate agrees well with the experimental finding that the coherent fraction make up 30–50% of the emission intensity in diamond.⁴ With the exceptions of the very shallow ones, the condition $\Gamma_c \gg \hbar\omega_D$ should be good for most of the core levels, and higher coherent fractions are expected. Finally, similar to the case of x-ray diffraction, thermal vibrations in the ground the final states should introduce a Debye-Waller factor in Eq. (4).

Multielectron effects will give rise to satellite structures in the emission spectrum and are incoherent because the emitted photon has different energy. They can be important for narrow band materials where the electron correlation effects are important,²⁰ or when the excitation energy is far above the absorption threshold. The multielectron effect can be included in Eq. (2) by using $S < 1$, which would further reduce the contribution of the coherent scattering in the total emission spectrum.

Some of the many-body effects can be studied with model Hamiltonians and perturbation theory. Suppose the e -ph or the e - e interaction is described by the interaction Hamiltonian, H_{int} , simple use of the first-order perturbation theory gives the following addition to the resonant transition amplitudes in Eq. (3):

$$\sum_n \frac{\langle f | \mathbf{p} \cdot \mathbf{A}_2 | n \rangle \langle n | H_{\text{int}} | m \rangle \langle m | \mathbf{p} \cdot \mathbf{A}_1 | i \rangle}{(E_m - E_n)(E_m - E_i - \hbar\omega_1 - i\Gamma_m/2)} .$$

This additional term can be used to study the excitation of a plasmon or phonon during the resonant scattering process. The conservation relations for these processes are modified to include the energy and momentum of the plasmon or phonons. In Fig. 2, we illustrate some of the scattering processes that may occur in the core state. The quantitative analyses of these processes are beyond the scope of this paper.

Having stated that XRES may be used as a band determination technique, we now discuss the advantages and limitations as compared to other band determination techniques such as the angle-resolved photoemission. Since only the detection and analysis of x-ray photons are used, XRES is bulk sensitive and has no problem with the sample charging effects associated with the electron detection techniques. Surface contamination and disorder will have a much smaller effect on the use of this technique. In addition, it can be used in external electric or magnetic fields. XRES has all the characteristics of absorption and emission spectroscopy, including the elemental, chemical, and the orbital symmetry sensitivity. Finally, because of the weak interaction between the emitted photon and the solid, the interpretation of the experiment is simpler than the photoemission process. This is in contrast to photoemission technique, where the escaping photoelectron interacts strongly with the solids, especially the surface, rendering it to be an essentially two-dimensional band mapping technique.

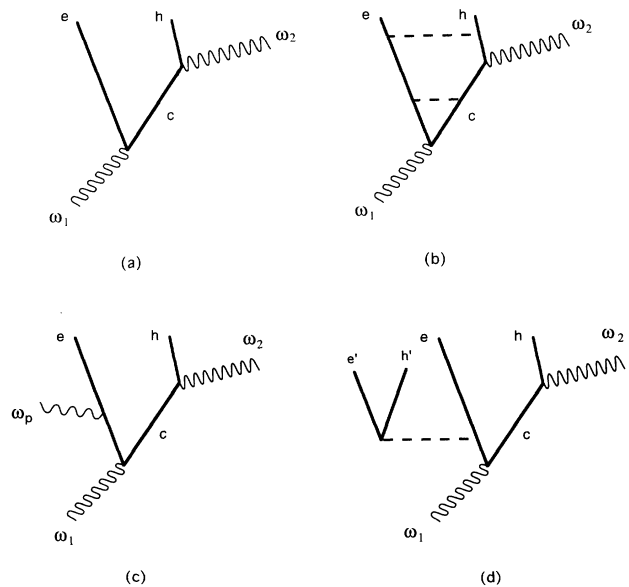


FIG. 2. Graphical illustration of selected relaxation processes during the XRES process. (a) No relaxation; (b) inclusion of the Coulomb interaction between the electron and the holes; (c) excitation of a plasmon or phonon with energy $\hbar\omega_p$ by the photoelectron (or the core hole); (d) excitation of an electron-hole pair by the photoelectron (or the core hole).

The disadvantages include the low detection efficiency, especially for soft x-ray photons, and the requirement for core levels with appropriate energies and small lifetime broadening. At x-ray energies of 5 keV or more, the natural width of the core levels can be more than 1 eV. This will limit the momentum resolution that can be achieved in the scattering experiments. The best region of study is therefore around x-ray energy of 2 keV, involving the resonant transition of the *K*-shell electrons of Si, S, etc. These core levels usually have fairly narrow natural widths and the x-ray wavelength is comparable to the usual lattice spacings.

It is interesting to note that there had been debate over "resonant scattering" (RS) or "absorption-followed-by-emission" (AE) description of resonant Raman scattering and hot luminescence in the visible region.²¹ It appeared that there has been no consensus as to whether the two descriptions are equivalent or not. Our discussion in the x-ray regime clearly shows that there is an observable difference between the RS and the AE approaches. The spatial coherence in the RS process yields diffractionlike effects that are absent from the AE picture. Note that this difference is only observable in solids or groups of atoms. If there is only one atom, the phase information from the absorption and emission processes in Eq. (4) will not manifest in the absolute cross section, and the RS and AE pictures are equivalent.

Finally, this work suggests that one should be careful when using the fluorescence yield technique to obtain the absorption spectra. Since the absorption-emission processes are correlated, the fluorescence technique may not yield the true absorption spectrum. A simple example of *L* edges of Mn²⁺ ion in, e.g., MnCl₂, in the ⁶S configuration illustrates the point. The *L* fluorescence is dominated by the radiative decay of the five *3d* electrons which are spin aligned. The fluorescence yield is only proportional to the excitation cross section whereby a *2p* electron with the same spin orientation as that of the *d* electrons is excited. In the other case when the absorp-

tion involves a *2p* electron with the opposite spin, the *3d* → *2p* radiative transition is not allowed due to the spin selection rule. Thus, in this example, the fluorescence yield technique only measures the partial absorption cross section.

IV. CONCLUSIONS

We have presented a general discussion of x-ray resonant inelastic scattering. The x-ray absorption-emission process is treated as a coherent inelastic scattering process where the incident photon loses energy to create an electron-hole pair. As a result of the momentum conservation in the scattering process, the valence-band emission spectra excited with monochromatic photon will, in general, be dependent on the excitation energy. Furthermore, it is possible to use the resonant inelastic scattering technique in the determination of both the occupied and unoccupied electron bands. This technique has some very attractive properties such as bulk sensitivity, charge neutrality, elemental specificity. Effects of the electron-electron and electron-phonon interactions are also considered. They contribute to the momentum resolution and the incoherent portion of the total scattering cross section, such as the excitation of phonons and plasmons. It is estimated that more than 50% of the total emission intensity may be due to the coherent process. With the development of the new generation of synchrotron radiation sources, this new understanding of the absorption and emission processes hopefully will stimulate more theoretical and experimental investigations on this new aspect of x-ray spectroscopy and yielding new spectroscopic technique for determining the electronic structures of materials.

ACKNOWLEDGMENTS

Insightful discussions with M. Blume, P. D. Johnson, S. D. Kevan, J. Nordgren, and E. A. Stern are acknowledged.

*Mailing address: Bldg. 510E, Brookhaven National Lab, Upton, NY 11973.

¹See, e.g., B. K. Agarwal, *X-Ray Spectroscopy* (Springer-Verlag, Berlin, 1991); A. Meisel, G. Leonhardt, and R. Szargan, *X-Ray Spectra and Chemical Binding* (Springer-Verlag, Berlin, 1989).

²See, for example, P. Cowan, *Phys. Scri.* **T31**, 112 (1990).

³N. Wassdahl *et al.*, in *X-Ray and Inner Shell Processes*, Proceedings of the X-90 Conference, AIP Conf. Proc. No. 215, edited by T. A. Carlson, M. O. Krause, and S. T. Manson (AIP, New York, 1990).

⁴Y. Ma, N. Wassdahl, P. Skytt, J. Guo, J. Nordgren, P. D. Johnson, J. E. Rubensson, T. Boske, W. Eberhardt, and S. Kevan, *Phys. Rev. Lett.* **69**, 2598 (1992).

⁵P. D. Johnson *et al.*, *Phys. Rev. B* **49**, 5024 (1994).

⁶J.-E. Rubensson, D. Mueller, R. Shuker, D. L. Ederer, C. H. Zhang, J. Jia, and T. A. Callcott, *Phys. Rev. Lett.* **64**, 1047 (1990).

⁷K. E. Miyano, D. L. Ederer, T. A. Callcott, W. L. O'Brien, J. J. Jia, L. Zhou, Q.-Y. Dong, Y. Ma, J. C. Woicik, and D. R. Mueller, *Phys. Rev. B* **48**, 1918 (1993).

⁸See, e.g., J. J. Sakurai, *Advanced Quantum Mechanics* (Addison-Wesley, Reading, MA, 1967), Chap. 2; see also, M. Blume, *J. Appl. Phys.* **57**, 3615 (1985).

⁹See, for example, W. Schulke, U. Bonse, H. Nagasawa, A. Kaprolat, and A. Berthold, *Phys. Rev. B* **38**, 2112 (1988), and references therein.

¹⁰C. J. Sparks, *Phys. Rev. Lett.* **33**, 262 (1974).

¹¹P. Eisenberger, P. M. Platzman, and H. Winick, *Phys. Rev. B* **13**, 2377 (1976).

¹²See, e.g., E. A. Stern and S. Heald, in *Handbook on Synchrotron Radiation*, edited by E.-E. Koch (North-Holland, Amsterdam, 1983), Vol. 1b, p. 955.

¹³More realistically, the core hole is viewed as localized. Using the atomic core wave functions located on individual atoms as the intermediate states will yield the same result in Eq. (4).

- ¹⁴P. Glans, P. Skytt, J. Guo, N. Wassdahl, J. Nordgren, and Y. Ma (unpublished).
- ¹⁵P. Skytt, P. Glans, J. Guo, N. Wassdahl, J. Nordgren, and Y. Ma (unpublished).
- ¹⁶Y. Ma, K. E. Miyano, P. L. Cowan, Y. Aglitskiy, and B. A. Karlin (unpublished).
- ¹⁷See, for example, F. Bassani and M. Altarelli, in *Handbook on Synchrotron Radiation*, edited by E.-E. Koch (North-Holland, Amsterdam, 1983), Vol. 1a, p. 463.
- ¹⁸W. L. O'Brien, J. Jia, Q. Y. Dong, T. A. Callcott, K. E. Miyano, D. L. Ederer, D. R. Mueller, and C. C. Kao, *Phys. Rev. Lett.* **70**, 238 (1983).
- ¹⁹C. O. Almbladh, *Phys. Rev. B* **16**, 4343 (1977); G. D. Mahan, *ibid.* **15**, 4587 (1977), and references therein.
- ²⁰N. Wassdahl *et al.*, *Phys. Rev. Lett.* **64**, 2807 (1990); J. J. Jia *et al.*, *ibid.* **67**, 731 (1991).
- ²¹M. V. Klein, *Phys. Rev. B* **8**, 919 (1973); Y. R. Shen, *ibid.* **9**, 622 (1974); J. R. Solin and H. Merkelo, *ibid.* **12**, 624 (1975).